International Journal of Thermophysics, Vol. 10, No. 5, 1989

Magnetic Rotating Disk Viscometer[1]

A. F. Borghesani[2] and M. Santini[2]

A rotating disk viscometer has been developed aiming at measuring the viscosity at the critical consolute point of binary mixtures in the true hydrodynamic limit. The viscometer consists of a small magnetized disk set into slow rotation by a uniformly rotating magnetic field. The liquid is continuously sheared and no frequency effects should manifest even at the critical point. The phase delay between field and disk depends on the torques acting on the disk, including that of viscous nature. The viscosity can be calculated from the knowledge of the viscous torque obtained after calibration of the viscometer using literature data for ethanol. Preliminary testing results obtained with this novel apparatus are reported.

KEY WORDS: critical consolute point; ethanol; 2-propanol; rotating disk viscometer; viscosity.

1. INTRODUCTION

Measurements of the shear viscosity of a binary liquid mixture should be made in the so-called "hydrodynamic limit," i.e., at a frequency $\omega \to 0$ and at a wavelength whose wave vector $\mathbf{k} \to 0$. However, if the characteristic time τ of the order parameter flulctuations and their characteristic length, the correlation length ξ, are such that fluctuations relax on a time scale much shorter than the characteristic time of the excitation, the liquid remains in equilibrium even in the presence of a macroscopic motion of the exciting body [1]. Therefore, in this case, shear viscosity measurements can be safely carried out at finite $\mathbf{k}$ and ω.

The critical consolute point, however, demands more stringent requirements on how viscosity has to be measured. Indeed, both the

[1] Paper presented at the Tenth Symposium on Thermophysical Properties, June 20–23, 1988, Gaithersburg, Maryland, U.S.A.

[2] Università degli studi di Padova, Dipartimento di Fisica "G. Galilei", Via F. Marzolo 8, I-35131 Padova, and GNSM/CISM, Padova, Italy.

0195-928X/89/0900-0917$06.00/0

correlation length ξ of the composition fluctuations and their characteristic lifetime τ diverge at the critical point according to the following power laws: $\xi \propto t^{-\nu}$ and $\tau \propto t^{-3\nu}$, where $t = (T - T_c)/T_c$ is the reduced temperature from the critical temperature and $\nu \approx 0.63$ is the critical exponent [2]. When measuring the shear viscosity at the critical consolute point, there will be a temperature range where both the conditions $k\xi < 1$ and $\omega\tau < 1$ are being violated. In particular, if $\omega\tau > 1$, the liquid will become viscoelastic, i.e., the fluid response is delayed with respect to the external excitation and the fluid will show a frequency dependent shear viscosity.

Moreover, another inequality has to be satisfied in order to approach sufficiently close the critical point without disrupting the characteristic fluctuations: $S\tau < 1$, where S is the shear rate. If the shear rate inequality is violated, both the viscoelastic behavior and an apparent change in the critical temperature are to be expected [3, 4].

In order to overcome these difficulties we have developed a novel continuously rotating disk viscometer. Its essential features are that the oscillation frequency, ω, is strictly zero (and, in any case, the rotation frequency is very low: 0.5–30 s^{-1}) and that the maximum shear rate can be varied at will over a wide range between $\approx 80 - 4800\ s^{-1}$. Viscosity variations as small as 0.1% can be easily detected. Other important features are its ruggedness and the ease of thermoregulation due to the small amount of sample to be used ($\leqslant 2\ cm^3$).

In this paper we describe the new viscometer and the calibration procedures, and we report the testing measurements carried out in a well-known simple liquid.

2. APPARATUS

The viscometer described here is a modification for measurements in liquids of a continuously rotating disk viscometer previously designed in our laboratory for accurate measurements at the critical point of the gas–liquid transition [5].

The new viscometer consists of a small, uniformly magnetized disk pivoted on ruby bearings. The disk is set into steady rotation by a uniformly rotating magnetic field **B**. The magnetic field is generated by two quadrature sinusoidal currents flowing in two pairs of coils wound around a soft iron torus (Fig. 1). The driving torque acting on the disk is given by

$$\tau_d = |\mathbf{M} \times \mathbf{B}| = MB \sin \phi \tag{1}$$

where **M** is the magnetic moment of the disk, **B** is the magnetic field, and ϕ is the phase angle between the magnetic field and the disk magnetization.

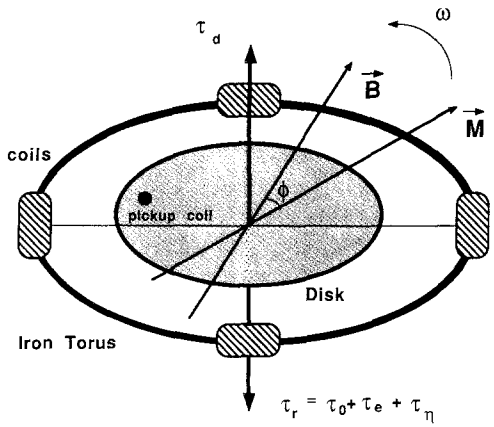

Fig. 1. Schematic drawing of the disk, the iron torus, the magnetic field generating coils, and the pickup coil.

The disk is also subjected to a retarding torque, τ_r , made up of three terms:

$$\tau_r = \tau_0 + \tau_e + \tau_\eta \tag{2}$$

The first term, τ_0, is due to the friction of the disk pivots on the ruby bearings and is independent of the angular disk velocity. The second one, τ_e, is of an electromagnetic nature and is due to the interaction of the disk magnetic moment with the eddy currents induced by itself in the metallic cell body. τ_e is therefore proportional to the angular disk velocity: $\tau_e = 2\pi K_e f$. Finally, the third term τ_η is that due to viscous friction.

The equation of motion of the disk is given by

$$-I\ddot{\phi}(t) = MB \sin \phi(t) - \tau_0 - \tau_e - \tau_\eta \tag{3}$$

where I is the inertia moment of the disk. Under steady-state conditions, one gets

$$MB \sin \phi = \tau_0 + \tau_e + \tau_\eta \tag{4}$$

The strength B of the magnetic field is proportional to the current intensity i flowing in the coils:

$$B = K_b i \tag{5}$$

By defining $i_0(f) = (\tau_0 + 2\pi K_e f)/MK_b$, $i_\eta = \tau_\eta / MK_b$, and $i_c = i_0 + i_\eta$, Eq. (4) becomes

$$\sin \phi = i_c / i \tag{6}$$

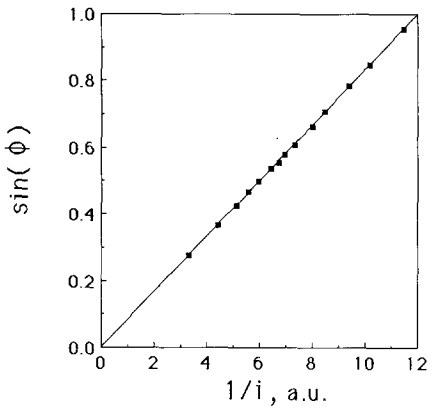

Fig. 2. Typical $\sin\phi - 1/i$ straight line. Its slope is the critical current.

By means of Eqs. (5) and (6) the torques acting on the disk are conveniently expressed in units of current.

For $i = i_c$ in liquid (or i_0 under vacuum), $\phi = \pi/2$. At such an angle the disk can no longer follow the magnetic field and stops. This current is therefore called the "critical current." The critical current i_c (or i_0) can be determined by fitting $\sin\phi$ vs the reciprocal of the field generating current intensity. A typical $\sin\phi - 1/i$ curve is reported in Fig. 2.

In vacuo, $\tau_\eta = 0$ and one gets

$$\sin\phi = i_0(f)/i \tag{7}$$

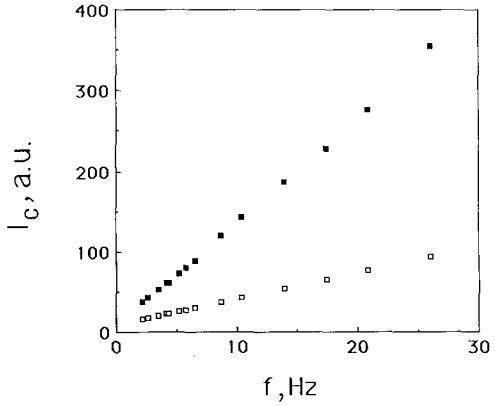

Fig. 3. Critical currents *in vacuo* (open squares) and in liquid ethanol (filled squares) at $T \approx 25°C$.

By fitting i_0 vs f one can separately determine both the mechanical and the electromagnetic contributions to the retarding torque.

In liquid, one has to take into account the viscous contribution i_η to the total torque. Now $i_c = i_0 + i_\eta$ depends also on the liquid properties. Typical results for the critical currents obtained *in vacuo* and in ethanol ($T \approx 25°C$) are shown in Fig. 3.

By subtracting the critical currents measured *in vacuo* to those measured in liquid one obtains the viscous torque contribution:

$$i_c - i_0 = i_\eta = \tau_\eta / MK_b \tag{8}$$

The viscosity η can be determined if one knows the relationship between the viscous torque and the viscosity, as explained next.

3. ELECTRONICS

3.1. Measurement of ϕ

To perform accurate viscosity measurements the angle ϕ must be determined very accurately. The motion of the disk is detected by a pickup coil located beneath it. The sinusoidal voltage signal appearing across the coil is amplified, squared, and compared with a similar signal derived from the field generating currents and, hence, in phase with the rotating field. The time delay T_ϕ between the two square waves is proportional to ϕ:

$$\phi = 2\pi f T_\phi \tag{9}$$

and is measured by means of conventional techniques.

To monitor ϕ as a function of time we have designed a "time difference-to-voltage converter" (Fig. 4). An S/R flip-flop (SRFF) is gated by the two square waves. Its output pulse of width T_ϕ controls the analog integration of a very constant current source ($1/I_0\, \Delta I_0/\Delta T \approx 5$ ppm $°C^{-1}$). At the end of the SRFF pulse the integrator output is sampled by a sample/hold circuit whose output V_ϕ, which is proportional to T_ϕ, is buffered, low-pass filtered, and read by a digital voltmeter. After the sampling procedure, the integrator is reset in order to repeat this measurement at each cycle.

The proportionality constant between V_ϕ and T_ϕ has been determined by feeding into this converter two voltage signals of variable frequency but with a fixed $\pi/2$ phase lag. The converter resolution is $\Delta\phi/\phi \approx 2 \times 10^{-4}$ and an overall accuracy of $\approx 1 \times 10^{-4}$ can be easily achieved by choosing adequate electronic components.

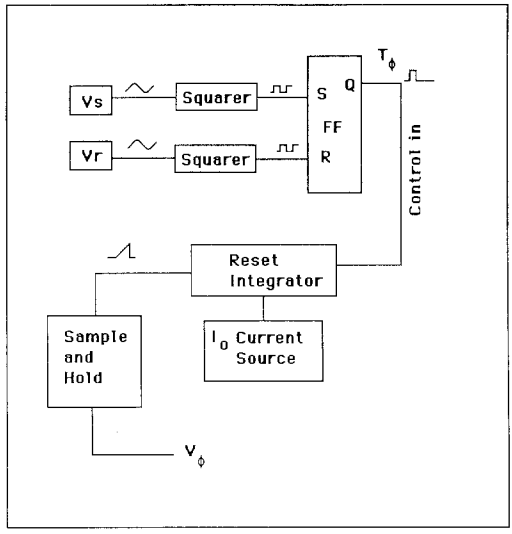

Fig. 4. Schematic electronic diagram of the "time difference-to-voltage" converter. V_s is the pickup coil signal and V_r is the reference signal.

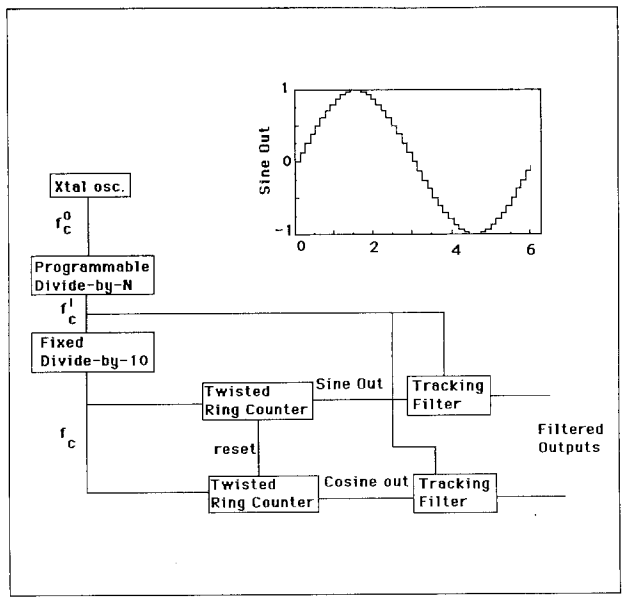

Fig. 5. Schematic electronic diagram of the sinusoidal waveform generators. The waveform before the tracking filters is shown in the inset.

3.2. Generation of the Rotating Field

The stability of the phase angle ϕ depends primarily on the frequency and amplitude stability of the rotating field. To generate it, two quadrature sinusoidal waveforms are needed to feed the coils wound around the iron torus. Although analog oscillators and phase-shifting networks are widely used, the several drawbacks shown by these circuits in the low-frequency region, especially if one wants to change the working frequency, are well known.

Therefore, we have designed a digital "sine-and-cosine wave" generator where both nonrecursive and recursive digital filtering techniques are exploited in order to obtain two sinusoidal waveforms whose $\pi/2$ phase shift and whose amplitudes turn out to be frequency independent. In Fig. 5 a simplified electronic diagram is shown. A high-frequency ($f_c^0 \approx 10^6$ Hz) quartz crystal CMOS oscillator gives the high-stability ($\Delta f/f <$ 1 ppm $°C^{-1}$) time base for all subsequent operations. Several cascaded programmable "divide-by-N" CMOS circuits allow scaling of the reference clock frequency down to the operating range.

After having divided f_c^0 by a suitable factor, we get a clock frequency f_c that clocks the operations of two similar 24-stage CMOS shift registers in twisted-ring-counter configuration. The binary waveform, obtained by feeding back the complemented output of the last stage to the DATA input of the shift register, is replicated at each output stage with a time delay of one clock period ($1/f_c$). By summing the first 23 outputs by means of a weighted resistors network the binary waveform is nonrecursively filtered, leaving the fundamental of frequency $f = f_c/48$ and of amplitude A plus higher-order harmonics of frequency $f_k = (48k \pm 1)f$ and of much lower amplitude $A_k = (48k \pm 1)^{-1}A$ for $k = 1, 2, \ldots$. The harmonic distortion as well as the amplitude ratios turn out to be frequency independent [6–8].

The resulting waveforms appears like a "staircase" made up of 48 steps. A reset signal is taken from the first ring counter after a quarter of a cycle in order to synchronize the second one with a delay of $\pi/2$, independent of the frequency. The output amplitude of these nonrecursive filters turns out to be temperature independent because of the small resistor loading of the CMOS output stage transistors.

The staircase-like signals are further smoothed by subjecting them to second-order low-pass digital recursive filtering by means of tracking filters [9], clocked at a frequency $f_c' = 10 f_c = 480 f$ that satisfies the Nyquist criterion [10]. By carefully adjusting the width of the sampling pulses of the tracking filters, the effective time constant for the two quadrature channels can be made equal.

The advantage of this filtering technique is that the filter cutoff

frequency is proportional to the fundamental frequency. It, therefore, automatically "tracks" changes of the fundamental frequency within a fraction of a period, adjusting itself in such a way that the filter attenuation and phase shift do not depend on the frequency. In the frequency range of interest, the $\pi/2$ phase difference between the two channels turns out to be constant to within 0.1% and the amplitude stability is within 0.3%. (It is worth recalling that the amplitudes can be accurately adjusted by means of potentiometric attenuators.)

Finally, the overall ϕ stability is of $\pm 0.05\%$ for over several weeks.

3.3. Thermostat

The thermostat (Fig. 6) is a conventional three-stage thermostat. An outer brass shield is thermoregulated to within $\approx 1°C$. An inner brass

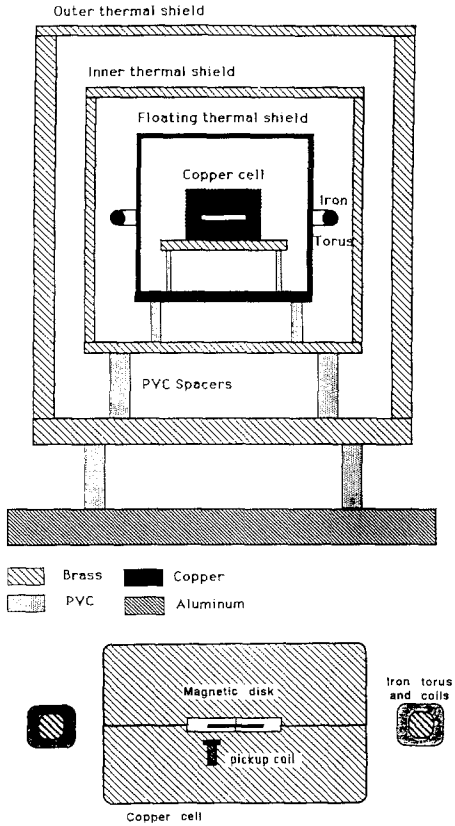

Fig. 6. Schematic drawing of the thermostat (top) and of the cell containing the rotating disk (bottom).

shield is thermoregulated to within $\approx 0.01\,^{\circ}C$ or better. A floating massive copper shield ensures that the cell "sees" an uniform temperature. The cell is finally thermoregulated to within $\pm 50\,\mu K$. AC ratio transformer bridges and thermistor sensors were used to measure the temperature [11].

4. TESTING MEASUREMENT RESULTS

The viscous torque is given by [12]

$$\tau_\eta = C\eta f y^{-1}(\delta) \tag{10}$$

where $\delta = (\eta/2\pi f\rho)^{1/2}$ is the boundary layer thickness and C is a geometrical factor. $y(\delta)$ has two limiting behaviors: $y \propto \delta$ for $\delta/Z_1 < 1$ and $y = 1$ for $\delta/Z_1 > 1$, where Z_1 is the distance between the disk surface and the top (or bottom) cavity surface. In our case $Z_1 = 0.025$ cm. From Eqs. (10) and (8) one has

$$y(\delta) = D\frac{\eta f}{i_c - i_0} \tag{11}$$

where $D = C/MK_b$ is a constant. We measured $i_c(f)$ in ethanol at $T = 25.1$ and $49.5\,^{\circ}C$. $i_0(f)$ was previously measured *in vacuo* at several temperatures. Viscosity and density of ethanol were interpolated from literature data [13]. The quantity $\eta f/(i_c - i_0)$ was then calculated and plotted vs δ. By normalizing it where it was constant to within 0.2%, we obtained the calibration constant D. In Fig. 7 the resulting $y(\delta)$ is reported

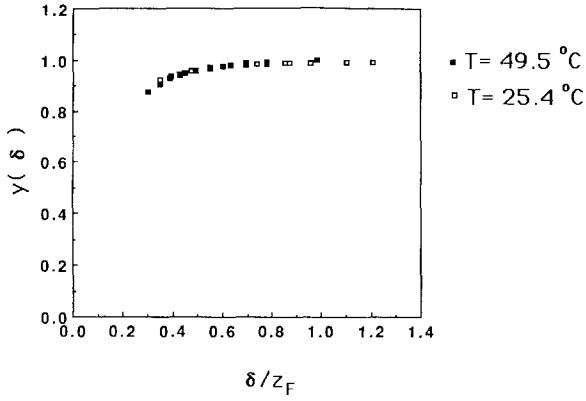

Fig. 7. The calibrating function $y(\delta)$ as a function of the boundary layer thickness scaled by the cell gap height. Calibrating liquid: ethanol. Open squares: $T \approx 25.4\,^{\circ}C$. Filled squares: $T \approx 49.5\,^{\circ}C$.

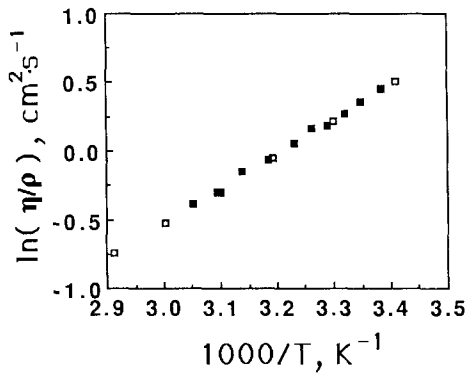

Fig. 8. Testing viscosity measurements in 2-propanol as a function of the reciprocal of the absolute temperature. Open squares: literature data. Filled squares: present data.

as a function of δ. We see that it is practically constant over a wide δ range. This means therefore that $\tau_\eta \propto \eta$ and does not depend on ρ.

To test our viscometer, we carried out measurements in 2-propanol in the range 22.5–55°C. Our results, shown in Fig. 8, compare very favorably with literature data [14] within the accuracy of the latter.

5. CONCLUSIONS

A novel type of viscometer for the liquid range has been described which allows viscosity measurements at zero oscillation frequency and should therefore be insensitive to viscoelastic effects close the critical consolute point of binary mixtures. The calibration procedure has been described. Comparison measurements in a known liquid are presented and show a very good agreement with literature data.

ACKNOWLEDGMENTS

We acknowledge useful discussions with Professor L. Bruschi. This work was sponsored by Consiglio Nazionale delle Ricerche and Ministero Pubblica Istruzione, Rome, Italy.

REFERENCES

1. J. C. Niewoudt and J. V. Sengers, *Physica* **147A**:368 (1987).
2. R. F. Berg and M. R. Moldover, *Int. J. Thermophys.* **7**:675 (1986).
3. R. F. Berg and M. R. Moldover, *Rev. Sci. Instrum.* **57**:1667 (1986).

4. R. F. Berg and M. R. Moldover, *J. Chem. Phys.* **89**:3694 (1988).
5. L. Bruschi, M. Santini, and G. Torzo, *J. Phys. E Sci. Instrum.* **17**:312 (1984).
6. J. Podolske, *Rev. Sci. Instrum.* **50**:1010 (1979).
7. H. Bachmair and R. Vollmert. *IEEE Trans. Instrum. Meas.* **IM-29**:370 (1980).
8. P. Horowitz and W. Hill, *The Art of Electronics* (Cambridge University Press, Cambridge, 1987), p. 448.
9. P. Horowitz and W. Hill, *The Art of Electronics* (Cambridge University Press, Cambridge, 1987), pp. 446–447.
10. H. Schmid, *Electronic Analog/Digital Conversions* (Van Nostrand Reinhold, New York, 1970).
11. L. Bruschi, M. Santini, and G. Torzo, *Rev. Sci. Instrum.* **56**:427 (1985).
12. A. F. Borghesani and L. Bruschi, *Z. Naturforsch.* **40a**:789 (1985).
13. *Handbook of Chemistry and Physics* (Chemical Rubber, Cleveland, 1949), pp. 1758, 1717.
14. *Beilsteins Handbuch der Organischen Chemie* (Springer-Verlag, Berlin, 1958), pp. 1441–1442.